JOURNAL OF THERMOPHYSICS AND HEAT TRANSFER
Vol. 17, No. 1, January–March 2003

Application of Magnetic Fluid Membrane for Flow Control

H. Yamaguchi,* Y. Suzuki,† and S. Shuchi‡
Doshisha University, Kyoto 610-0321, Japan

To study the application of a magnetic fluid membrane for flow rate control, an experimental investigation was conducted to obtain the basic characteristics and to verify the feasibility of practical use. The working principle of a magnetically controlled magnetic fluid membrane is based on the magnetic attraction body force exerted on the magnetic fluid, which is sustained in the cross-sectional area of a pipe. In the experiments, rupture pressure was obtained at various conditions for an oil–magnetic fluid interface. Also, from the results obtained for the flow rate ontrol characteristics, it was found that the magnetically controlled membrane has a function similar to that of an ordinary butterfly valve, and it was shown that the membrane would be feasible for controlling lower flow rates at lower driving pressure gradients.

Nomenclature

D	=	circular valve diameter of butterfly valve, m
D_0	=	pipe diameter of butterfly valve, m
d	=	pipe diameter of test section, m
H	=	magnetic field intensity, A/m
$\boldsymbol{H}$	=	magnetic field vector
H_r	=	intensity of magnetic field in r direction, A/m
H_z	=	intensity of magnetic field in z direction, A/m
$(H_z)_{\max}$	=	maximum of H_z, A/m
I	=	applied dc current, A
l	=	pipe length, m
l_e	=	effective length, m
l_m	=	length covered by magnetic fluid, m
M	=	magnetization, Wb/m^2
$\boldsymbol{M}$	=	magnetization vector, Wb/m^2
P_{loss}	=	pressure loss, Pa · s
P_r	=	rupture pressure, Pa · s
Re	=	Reynolds number
r, θ, z	=	cyclindrical coordinates (see Fig. 6)
V_m	=	volume of sustained magnetic fluid, m^3
v	=	area mean velocity, m/s^2
ΔP	=	measured pressure difference, Pa
δ	=	valve opening angle of butterfly valve, rad
ε	=	pressure loss coefficient
η	=	test fluid viscosity, Pa · s
λ	=	friction loss coefficient ($\lambda = 64/Re$)
ρ	=	working fluid density, kg/m^3

I. Introduction

A MAGNETIC fluid is a colloidal suspension of 10-nm ferromagnetic particles that are suspended with a surfactant coating in a carrier liquid such as hydrocarbon, ester, or water.[1–3] Magnetic fluid behaves as an electrically nonconducting homogeneous media in which single-domain magnetic particles are stabilized even in strong magnetic fields. Because magnetic fluids have magnetic properties along with fluidity, many applications have been proposed to date, such as magnetic seals, dampers, bearings, etc.[1–3] Among the many promising technological applications of magnetic fluids are those devices that use surface deformation with magnetic attraction force.

A unique application for an aperture control, which is derived from the interfacial formation of magnetic fluid, was proposed in our previous research work.[4] The basic results were presented for a sustained magnetic fluid membrane in a pipe section under an applied magnetic field. In view of possible engineering applications, detailed characteristics were reported in Ref. 4 for the formation process and the aperture variation in terms of imposed magnetic field intensity.

In the present study, which proceeds from our previous study,[4] a new method of flow rate control that uses sustained magnetic fluid in a pipe under an applied magnetic field is proposed. The basic idea of using the sustained magnetic fluid in a section of a pipe is to form the membrane and block the passage of flow by controlling magnetic field intensity. In the present investigation, the rupture pressure of the membrane (which is analogous to the holding pressure of an ordinary mechanical flow control valve) is investigated experimentally, using a water-based magnetic fluid (W-40) with a working fluid of mineral oil. In the experiment, the rupture pressure of the magnetic fluid membrane for varying magnetic field intensity is recorded for a given volume of magnetic fluid sustained in the pipe section. While controlling the volume flow rate of the working liquid (oil), the flow characteristics (the pressure loss coefficient across the membrane) are also recorded and examined to simulate a flow control valve.

II. Experimental Apparatus and Procedure

Figure 1 is a schematic diagram of the experimental apparatus. In the present investigation, oil, whose physical properties are presented in Table 1, is used as a test working fluid. To drive the working fluid into the test section, the working fluid, which is contained in the cylinder, is forced to flow by inward pushing of the piston with driving units that consist of an electric motor, speed controller, and other mechanical parts, as shown in Fig. 1. In this investigation, the pressure and volumetric flow rate are kept constant throughout the experiments. The volumetric flow rate of the working fluid was obtained by knowing the speed and area of the piston. Differential pressure across the test section, which is used to obtain to the pressure loss coefficient, was measured by the differential pressure gauge, as indicated in Fig. 1. The inlet length to the test section was taken sufficiently long so that the flow coming into the test section was a fully developed steady laminar pipe flow. The test section is made of acrylic pipe with an inner diameter of 12 mm and total length of 800 mm, where a given volume of magnetic fluid is sustained by a magnetic field forming a membrane. A cylindrical coil electromagnet is placed around the test section, and it is cooled by circulating water from a cooler unit. The electromagnet is powered by a dc power supply unit, capable of producing a magnetic field

Received 12 April 2002; revision received 22 July 2002; accepted for publication 24 July 2002.

*Professor, Department of Mechanical Engineering; hyamaguc@mail.doshisha.ac.jp.

†Research Student, Department of Mechanical Engineering; eta1305@mail4.doshisha.ac.jp.

‡Research Student, Department of Mechanical Engineering; dta0379@mail4.doshisha.ac.jp.

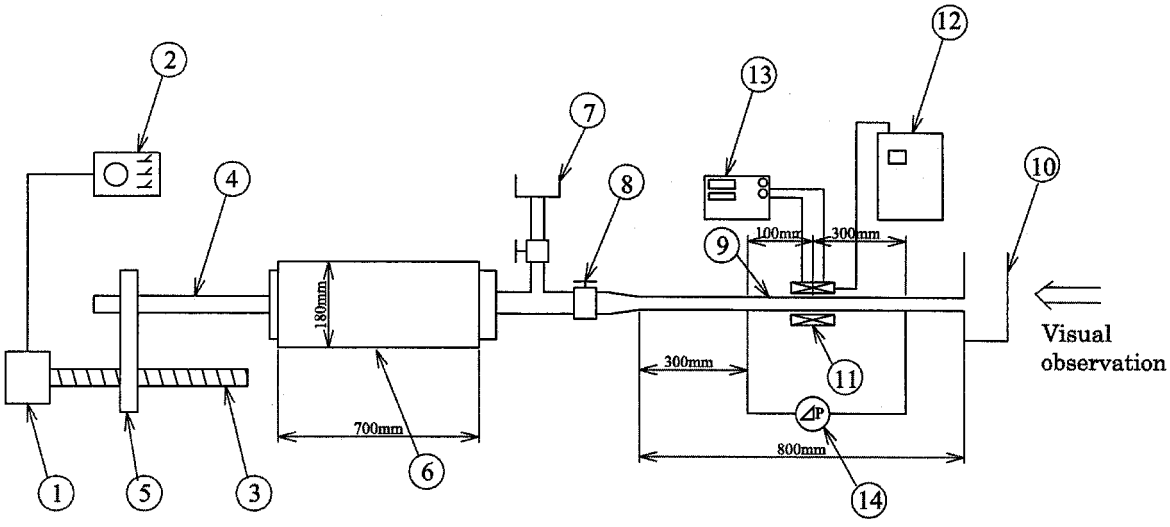

Fig. 1 Experimental apparatus: 1, electric motor; 2, speed controller; 3, ball screw; 4, piston rod; 5, coupling plate; 6, cylinder; 7, filler tank; 8, flow valve; 9, test section; 10, tank; 11, electromagnet; 12, cooler; 13, dc power supply; and 14, differential pressure gauge.

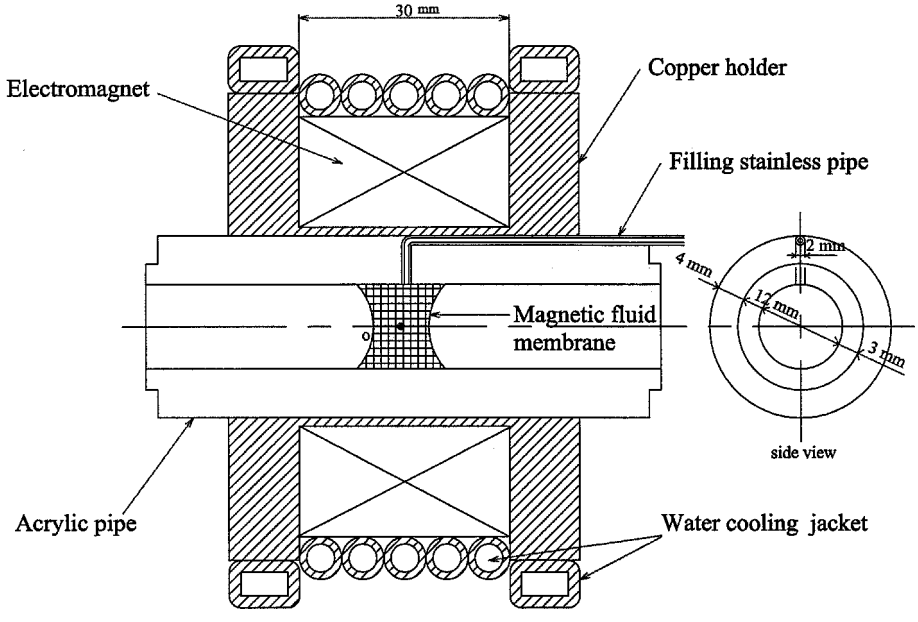

Fig. 2 Details of test section.

strength of $0 \sim 0.50 \times 10^5$ A/m in the test section. A visual observation was also conducted during each flow test to obtain visual information regarding the surface of the magnetic fluid membrane under the magnetic field. The visual observation was done by viewing the test section from the side of the reservoir tank as shown in Fig. 1.

The arrangement of the test section is basically the same as in the previous investigation.[4] In Fig. 2, details of the test section are shown. Before each flow experiment, exact experimental conditions were set first by pouring the working fluid into the cylinder through the filler tank (as shown in Fig. 1). Then a given volume of magnetic fluid was inserted into the test section by a syringe through the stainless filling pipe as shown in Fig. 2, while an appropriate magnetic field to sustain the magnetic fluid in the test section was applied. Experiments were carried out in a temperature controlled room so that the physical properties (Table 1) of the working fluid and magnetic fluid were kept constant at 25°C(±1°C). For a given volume of magnetic fluid, the magnetic field was varied where the externally applied magnetic field was imposed on the membrane by the coil electromagnet, which is held in a copper holder as shown in Fig. 2. Before the flow experiments, without the presence of working fluid and magnetic fluid, detailed data were recorded for magnetic field distribution in the test section by supplying dc electric power to the magnet. In Figs. 3 and 4, representative distributions of the magnetic field intensity in the test section are plotted for the axial component H_z and for the radial component H_r, respectively. In Fig. 5, the normalized axial magnetic field intensity $H_z/(H_z)_{\max}$ is plotted for the axial coordinate z in the test section when a typical dc current of $I = 100$ mA was applied to the magnet. As seen in Fig. 5, there is a smooth and symmetric magnetic field for H_z^*, which is the normalized value with the peak value occurring at $z = 0$ (which varies for the r direction and zero value of H_r at $z = 0, r = 0$). Note from Figs. 3 and 4 that the magnetic fields are symmetric because the magnetic field was generated by the solenoid coil electromagnet.

The distribution of the magnetic field intensity was measured by a Hall probe, whose instrumentation accuracy is within ±1% for the range of magnetic field intensity. However, the largest measurement error comes from positioning the Hall probe in the measuring space, which was achieved by constructing a procession stage. The margin of error associated with the measurement of the magnetic field

Table 1 Properties of test fluids at 25°C

Test fluid	Density, kg/m^3	Viscosity, Pa · s
Mineral oil SM-2	0.832×10^3	1.86×10^{-3}
Magnetic fluid W-40	1.407×10^3	30×10^{-3}

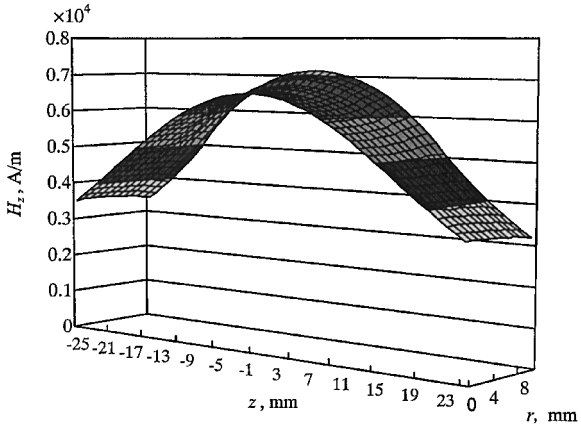

Fig. 3 Distribution of magentic field $H_z/(H_z)_{max}$.

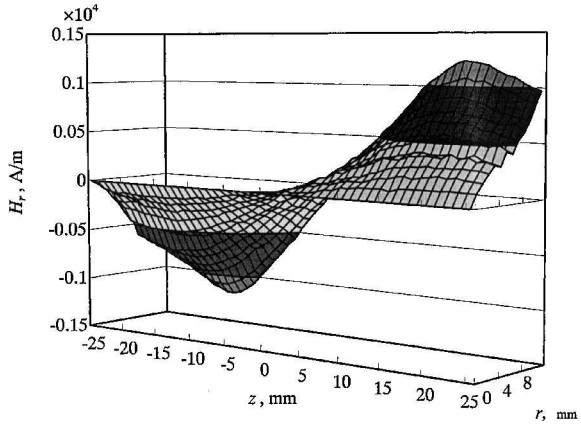

Fig. 4 Distribution of magentic field $H_r/(H_r)_{max}$.

intensity is approximately a maximum of ±4.0%. The procedure of the measurement (positioning the Hall probe) was repeated several times to minimize the error. The data shown in Figs. 3–5 are the average values from repeated measurements.

In Fig. 6, a schematic diagram describing the sustained magnetic fluid membrane with applied magnetic field $\boldsymbol{H}$ is shown, with the cylindrical coordinate system also presented. The origin o of the coordinate system, as shown in Fig. 6, is taken at the center of electromagnet on the axis of the pipe in the test section. Note that pressure measurements were made by differential pressure transducers both during the static experiment, where the rupture pressure across the membrane was recorded, and during the flow experiment, where the pressure difference across the membrane was recorded.

The magnetic fluid used in the present investigation was a water-based magnetic fluid (W-40) as supplied by industry. Its magnetization characteristic is displayed in Fig. 7, where the curve is well expressed by the Langevin function (see Ref. 5). The working fluid is mineral oil SM-2 as supplied by industry with the properties shown in Table 1. The mineral oil provides excellent separation from the magnetic fluid.

The measurement error associated with the pressure difference and the rupture pressures purely comes from the instrumentation accuracy, which has a maximum of approximately ±1.5%. The measurement of the recorded magnetic field distribution and the intensity involved certain human measuring errors, although the field was measured by a Hole probe with a precision coordinate table. The error associated with measuring the magnetic field distribution and

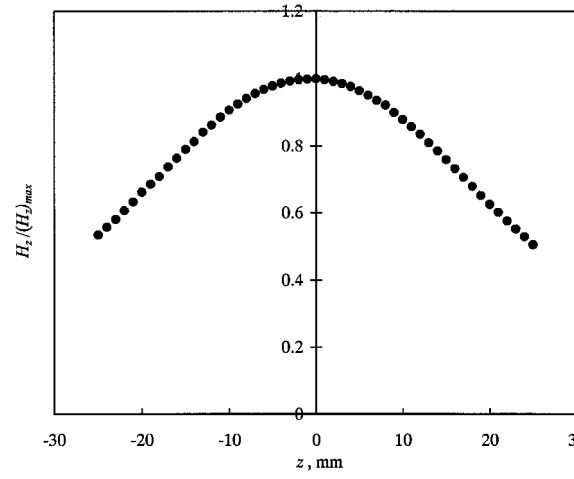

Fig. 5 Normalized axial magnetic fluid intensity.

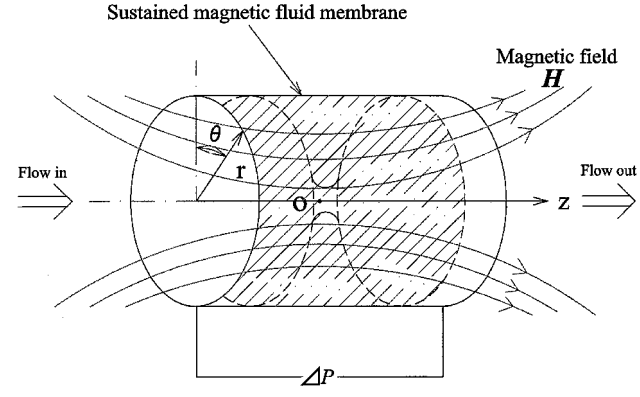

Fig. 6 Cylindrical coordinate system for applied magnetic field H.

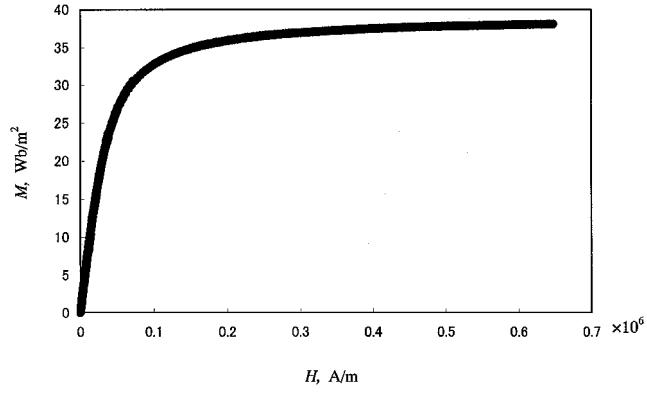

Fig. 7 Magnetization characteristics of magnetic fluid W-40.

intensity would be approximately maximum ±4.0% due to certain uncertainty in determining the exact space position. The sustained volume of the magnetic fluid was measured by a fine syringe scale with a maximum possible error of ±3.0%. The determination of volume flow rate of the working fluid had some uncertainty involving measuring piston speed, particularly at lower piston speed, due to friction of the ball screw at lower torque. The volume flow rate measurement error by repeated measurements would be approximately ±5 ~ 7% maximum.

III. Results and Discussion

A. Rupture Pressure

Before flow rate controlling characteristics were examined, the rupture pressure was obtained for various magnetic field intensities. The rupture pressure is the critical pressure difference when

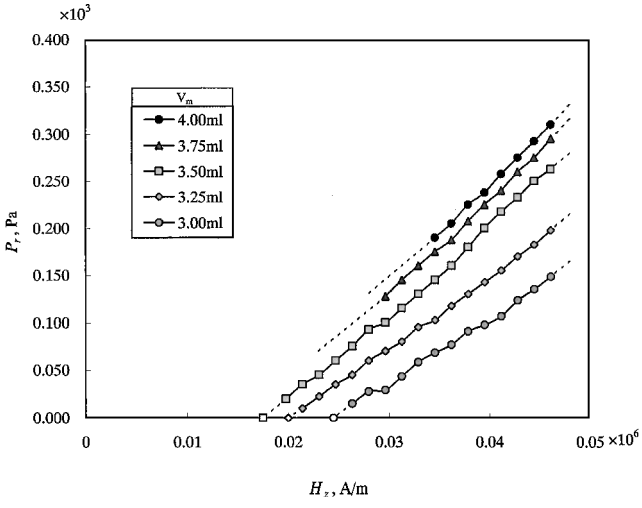

Fig. 8 Rupture pressure (oil–magnetic fluid).

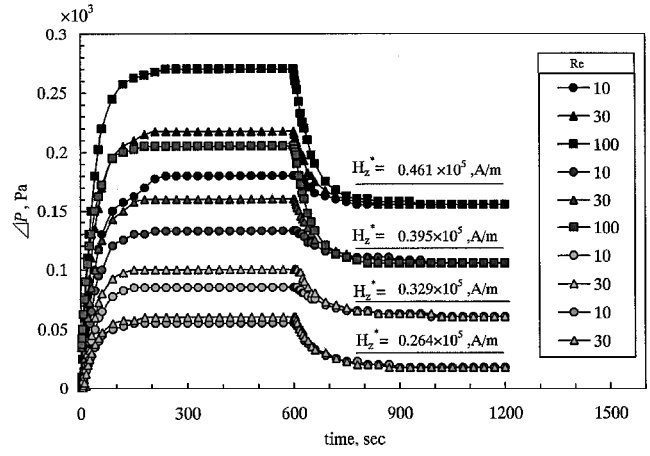

Fig. 9 Transient behavior of ΔP across magnetic fluid membrane, $V_m = 3.00$ ml.

the magnetic fluid membrane is broken by applying a pressure difference across the interfacial surface of the membrane. Figure 8 shows the results of rupture pressure P_r against magnetic field intensity H_z^* for given sustained volume of magnetic fluid. As can be seen from Fig. 8, the rupture pressure increases linearly with applied magnetic field intensity. Also, the rupture pressure becomes higher when the sustained volume is increased. With a higher sustained volume, such as $V_m = 4.00$ and 3.75 ml in Fig. 8, the thickness of membrane (particularly toward the lower wall region) was spread over the measuring section (over the width of the electromagnet) when magnetic field intensity was reduced (for example, $H_z^* \leqq 0.35 \times 10^5$ A/m for $V_m = 4.00$ ml), due to the gravity force, so that data were not recorded. However, when a lower sustained volume is used, such as $V_m = 3.00$, 3.25, and 3.50 ml in Fig. 8, and the magnetic field intensity is reduced, the membrane can be ruptured (or opened) only by applying the magnetic field without a pressure difference across the membrane, shown in Fig. 8 as points on the H_z^* axis for $P_r = 0$. The formation process of the membrane without pressure difference is fully discussed in Ref. 4.

B. Pressure Loss Coefficient

With regard to controlling the flow rate with the membrane by applying a magnetic field, the pressure drop across the membrane was measured when the working fluid started to flow through the ruptured (opened) hole. In the present study, the pressure loss coefficient across the membrane was obtained for a given sustained volume of magnetic fluid with the effects of magnetic field intensity H_z^* and Reynolds number,

$$Re \equiv \rho v d/\eta \tag{1}$$

for dimensionless volume flow rate of the working fluid. The pressure loss coefficient ε is defined as follows:

$$\varepsilon = (\Delta P - P_{\text{loss}}) \Big/ \tfrac{1}{2}\rho v^2 \tag{2}$$

where v is given for the working fluid. P_{loss} is the pressure loss due to wall friction, as follows:

$$P_{\text{loss}} = \lambda(le/d) \cdot \tfrac{1}{2}\rho v^2 \tag{3}$$

where λ is given for the pipe. It is noted that, for Eqs. (2) and (3), $d = 12$ mm and l_e is the effective pipe length between positions of differential pressure transducers defined as $l_e = l - l_m$ ($l = 400$ mm). Also note that l_m, the distance covered by the magnetic fluid in the section of the pressure measurement, was subtracted from l in Eq. (3). This was done in determining ε in Eq. (2), though the pressure loss associated with the distance l_m was effectively less than the maximum 0.08% in the range of Reynolds number used in the present study.

Figure 9 shows transient behavior of pressure difference ΔP for some representative Reynolds numbers. In Fig. 9, for the sake of comparison, the sustained volume was kept constant at $V_m = 3.00$ ml, and the Reynolds number was varied for each given magnetic field intensity H_z^*. The diagram shows the readings of the differential pressure output ΔP as time elapses after the fluid is suddenly driven to flow at a constant speed by the pushing piston. It is seen in Fig. 9 that as the magnetic field becomes higher, the magnitude of the startup transition for ΔP becomes larger. Also, for higher Reynolds numbers, such as $Re = 100$ (at $H_z^* = 0.461 \times 10^5$ A/m), the magnitude of the startup transition for ΔP becomes larger, that is, with a higher magnetic field the rupture pressure is high (as already seen in Fig. 8), thus, ΔP becomes high. The startup transition is caused after the rupture of membrane when the aperture area starts to expand as the working fluid flows through the opening area as time elapses. When the aperture area becomes constant with increasing time, the opening of the aperture reaches steady state, resulting in ΔP reaching a plateau, the steady state, as seen in Fig. 9. Note that for the lower magnetic field case, such as $H_z^* = 0.264 \times 10^5$ A/m in Fig. 9, the dependency of the transient behavior on Reynolds number becomes small. This is mainly because, with small magnetic field intensity, the effect of magnetic body force[1] becomes small due to the very small rupture pressure, so that the effect of the volume flow rate, that is, Reynolds number and inertia, in opening the aperture area wider becomes minimal. As seen in Fig. 9, at 600 s after the startup the movement of piston was suddenly stopped to verify the decay transition of ΔP. When the flow through the aperture area of the membrane is ceasing, the aperture area tends to close itself and then finally reaches a completely closed state, where the pressure difference ΔP reaches the value of the rupture pressure. Thus, in the present investigation, the decay plateau has implications on the rupture pressure, as seen in Fig. 8.

The control of volume flow rate (flow rate control characteristics) by the membrane of the sustained magnetic fluid is represented by a relationship between the pressure loss coefficient ε [Eq. (2)] and Reynolds number (volume flow rate), much like ordinary mechanical flow control valves.[6] In Figs. 10–14, the flow rate control characteristics are presented for different sustained volumes of magnetic fluid, and, in each case, the magnetic field intensity is varied. As seen in Figs. 10–14, the pressure loss coefficient ε decreases as Reynolds number Re is increased, where ε can be increased by applying a higher magnetic field intensity. There are strong dependencies of the sustained volume of magnetic fluid on the flow rate control characteristics, as seen in Figs. 10–14. With higher sustained volumes of magnetic fluid, such as 3.75 and 4.00 ml (Figs. 13 and 14), ε increases substantially. Thus, with a higher sustained volume and the application of a higher magnetic field intensity, the membrane could control a higher range of applied pressure with a higher volume flow rate. This results from a higher magnetic body force caused by the higher volume and an applied higher

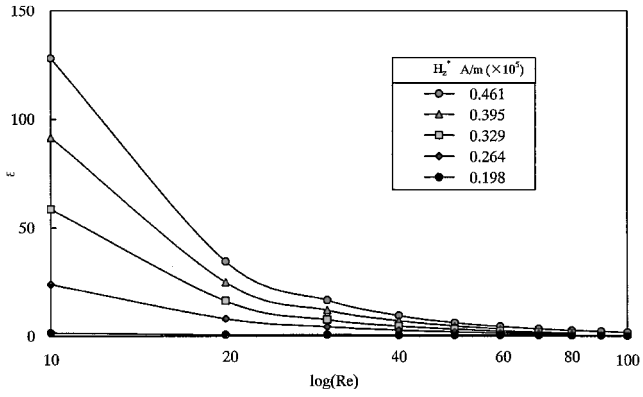

Fig. 10 Pressure loss coefficient for oil–magnetic fluid at $V_m = 3.00$ ml.

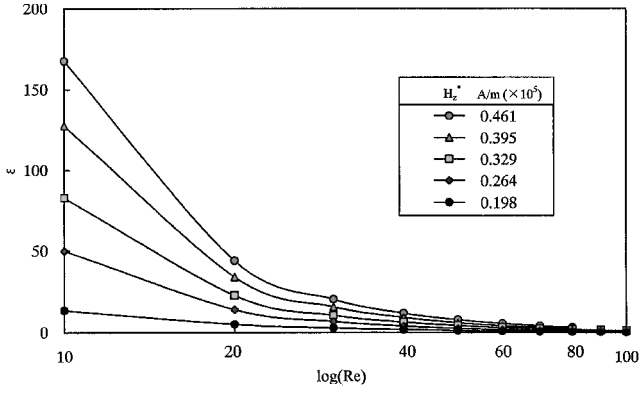

Fig. 11 Pressure loss coefficient for oil–magnetic fluid at $V_m = 3.25$ ml.

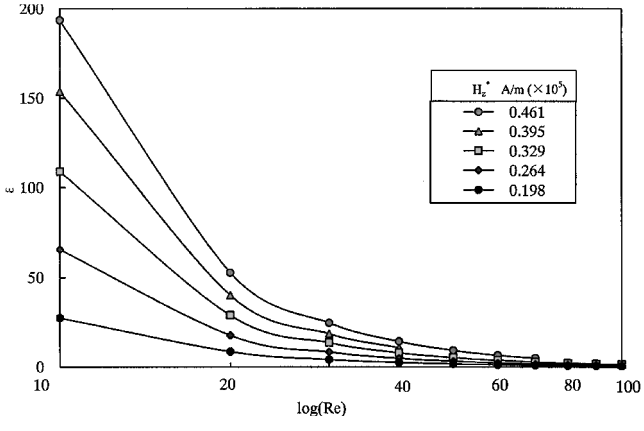

Fig. 12 Pressure loss coefficient for oil–magnetic fluid at $V_m = 3.50$ ml.

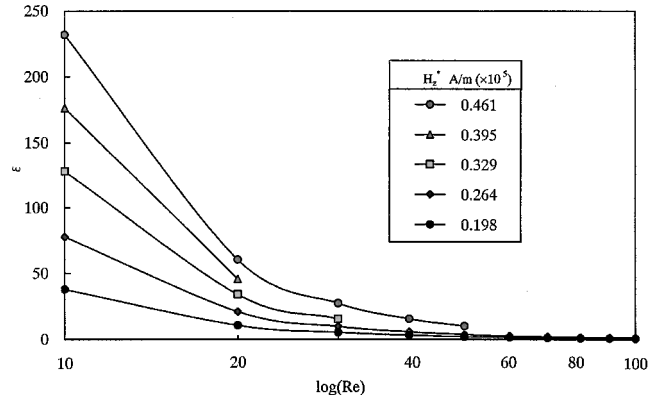

Fig. 13 Pressure loss coefficient for oil–magnetic fluid at $V_m = 3.75$ ml.

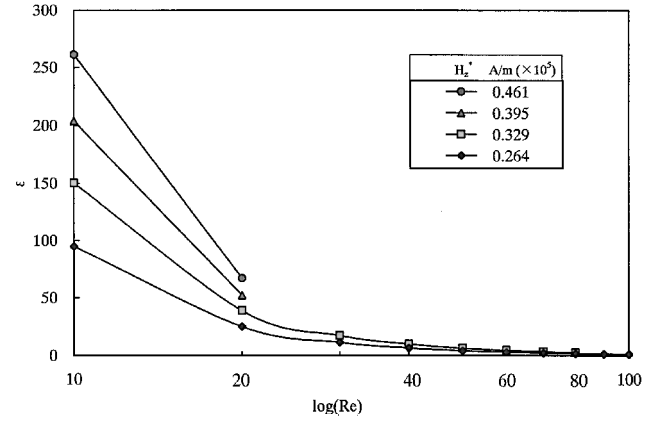

Fig. 14 Pressure loss coefficient for oil–magnetic fluid at $V_m = 4.00$ ml.

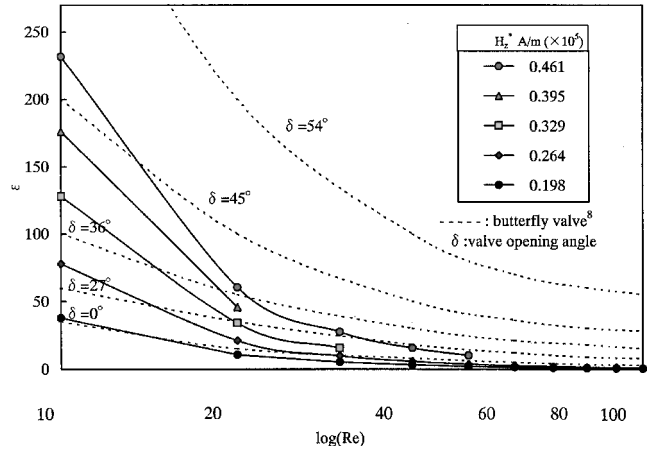

Fig. 15 Comparision of membrane flow control characteristic to that of butterfly valve, $V_m = 3.75$ ml.

magnetic field intensity that holds the membrane's shape[4] against the applied pressure across the membrane. Note that the discontinuity of data points, such as that seen for $H_z^* = 0.461 \times 10^5$ A/m in Fig. 13 and for $H_z^* = 0.41 \times 10^5$ A/m and $H_z^* = 0.395 \times 10^5$ A/m in Fig. 14, indicates the breaking up points of the membrane. At these breaking up points, for an associated Reynolds number, the surface around the aperture area (the opening edge) tends to break up into droplets and flow away with the stream of working fluid. The breaking up probably occurs due to a surface instability based on the Kelvin–Helmholtz instability[1] of the contact interfacial surface. Thus, this breaking up phenomenon would impose limitations on the utilization of the membrane for controlling volume flow rate. The surface instability[1–3] is another important surface phenomenon of the magnetic fluid membrane to consider. However, in the range of the magnetic field intensity used in the present investigation, $0 \leqq H_z^* \leqq 0.461 \times 10^5$ A/m, the surface instability was not observed by the visual observation before the breaking up. Thus, the interfacial instability due to the Kelvin–Helmholtz instability would be the major cause for the breaking up phenomena in the range of the magnetic field intensity in the present study.

Also note that the membrane for an air working fluid (the air–magnetic fluid interface) would not function in controlling the volume flow rate. This is due to bubbling from the membrane when the air is passed through the aperture area, a phenomenon that is also observed in soap bubbles. It is thought that the surfactant used as a coating substance to disperse the magnetic particles is responsible for the bubbling phenomenon.[7]

Finally, in Fig. 15, the flow rate controlling characteristic of the membrane for a representativecase, $V_m = 3.75$ ml, is compared with a typical butterfly valve (see Appendix).[8] Although there would not be any reason for a direct comparison with the mechanical butterfly valve, there exists a similarity in the controlling of the volume flow rate. In the Appendix δ is the opening angle of the butterfly valve,

and it exhibits a similar effect as that of the applied magnetic field intensity, although the controlling range for the membrane is rather limited at a lower Reynolds number in this comparison. The chief advantage as opposed to an ordinary butterfly valve is that the action of closing and opening valve can be achieved directly by applying the magnetic field to the sustained magnetic fluid, resulting in a rapid response, whereas with the butterfly valve, the action of closing and opening the valve is usually done by a servomechanism. In addition, it is thought that the magnetically controlled membrane would be more appropriate for controlling low flow rate gases with an accurate and fine flow control characteristic.

In the present investigation, the basic characteristic of controlling the volume flow rate with a magnetically sustained membrane was presented for application as a flow control device. Because the response time of forming the membrane when the magnetic field intensity is altered is on the order of 10^{-6} s (the typical relaxation time of the magnetic fluid),[1] the action of controlling the flow would be superior to ordinary mechanically controlled flow valves. Note that magnetic rheological (MR) fluid is another interesting smart fluid for possible utilization in flow control such as that proposed in the present study because the magnetization is usually much higher than the magnetic fluid. A detailed study of a magnetically controlled MR fluid membrane is forthcoming. As stated earlier, the working fluid (mineral oil SM-2; Table 1) provides excellent separation of the magnetic fluid, and the magnetization characteristics of the magnetic fluid did not change with repeated usage in the present experiment. However, long-term degeneration would occur, and the problem, including evaporation of the carrier liquid of the magnetic fluid in the event of air contact, must be considered in a practical industrial use. Much attention and improvement would be required for more practical uses, but the feasibility of a magnetically sustained membrane is verified in the present study.

IV. Conclusions

A study to investigate the use of a magnetically sustained membrane of magnetic fluid for controlling volume flow rate was carried out experimentally. From the experimental results, the following conclusions were drawn:

1) The rupture pressure (which implies the valve holding pressure in an ordinary flow control device) has an almost linear relationship with applied magnetic field intensity. For a higher sustained volume of magnetic fluid, the rupture pressure is higher.

2) The pressure loss coefficient ε is a decreasing function of increasing Reynolds number Re in the flow rate controlling characteristic of the membrane. For a higher sustained volume of magnetic fluid, the flow rate controlling characteristic (ε–Re relation) is greater, and it has a trend similar to that an ordinary butterfly valve. The feasibility of utilizing the membrane as a flow control device was positively verified.

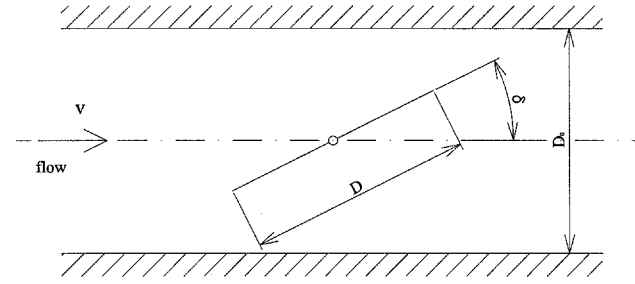

Fig. A1 Schematic of butterfly valve.

Appendix: Butterfly Valve

Figure A1 shows a typical butterfly valve, where the circular valve of diameter D is situated in the middle of a pipe whose diameter is D_0; δ is the valve opening angle. Reynolds number Re is defined as $Re = \rho v D_0/\eta$, where is v the area mean velocity.

Acknowledgment

This work was partly supported by a Grant-in-Aid for Scientific Research (Category C) from the Japan Ministry of Education, Culture, Sports, Science, and Technology.

References

[1]Rosensweig, R. E., *Ferrohydrodynamics*, 1st ed., Cambridge Monographs on Mechanics and Applied Mathematics, Cambridge Univ. Press, New York, 1985, pp. 1–8, 61–63, 110–119, and 202–206.

[2]Berkovsky, B. M., Medvedev, F. V., and Krakov, M. S., *Magnetic Fluids Engineering Applications*, Oxford Univ. Press, New York, 1993, pp. 1–24.

[3]Blums, E., Cebers, A., and Maiorov, M. M., *Magnetic Fluids*, 1st ed., Walter de Gruyter, New York, 1997, pp. 343–375.

[4]Yamaguchi, H., Suzuki, Y., and Shuchi, S., "Membrane Formation Process in Magnetic Fluid and Application for Aperture Control," *Journal of Thermophysics and Heat Transfer* (to be published).

[5]Chantrell, R. W., Popplewell, J., and Charles, S. W., "Measurements of Particle Size Distribution Parameters in Ferrofluids," *IEEE Transactions on Magnetics*, Vol. 14, No. 5, 1978, pp. 975–977.

[6]Joseph, A. S., and Allen, E. F., "Geometric Characteristics of Selected Valves," *Handbook of Fluid Dynamics and Fluid Machinery*, Vol. 3, Applications of Fluid Dynamics, Wiley-Interscience, New York, 1996, pp. 2043–2054.

[7]Jacob, N. I., *Intermolecular and Surface Force*, 2nd ed., Academic Press, London, 1992; Asakura Book Corp., Ltd., Tokyo, 1996, pp. 301–325 (Japanese translation).

[8]Murata, S., and Miyake, Y., *Hydrodynamics*, Rikogakusha, Tokyo, 1982, pp. 65–67 (in Japanese).